RUSSIAN JOURNAL OF EARTH SCIENCES, VOL. 15, ES1004, doi:10.2205/2015ES000550, 2015

Pyroxenite xenoliths in basalts of the Roca Negra volcano, Catalonia

A. F. Grachev[1]

Received 17 May 2015; accepted 22 May 2015; published 10 June 2015.

Newly obtained data on the whole-rock, trace-element, and He, Sr, and Nd isotopic composition of xenoliths in basalts of the Roca Negra Quaternary volcano in Catalonia, Spain, are used in discussing the problem of mantle metasomatism that produced pyroxenite xenoliths of unusual mineralogical and isotopic-geochemical composition. *KEYWORDS:* Xenoliths; basalt; mantle metasomatism; chemical geodynamics; Catalonia.

Citation: Grachev, A. F. (2015), Pyroxenite xenoliths in basalts of the Roca Negra volcano, Catalonia, *Russ. J. Earth. Sci., 15,* ES1004, doi:10.2205/2015ES000550.

Introduction

The Roca Negra volcano is a monogenic cinder cone in Catalonia, northeastern Spain, where young volcanic rocks are known to occur within a relatively small area. Basalt outcrops cluster in three fields: Garrotxa (Olot), Ampurdan, and Selva (Figure 1). The first K–Ar dates of the rocks led Donville [*Donville*, 1973] to distinguish three episodes of magmatism in this area: at 10–7.7 (Ampurdan), 5.5–2.0 (Selva), and < 0.11 Ma (Garrotxa). However, these dates seem to reflect the discreteness of the age values rather than the actual discreteness of pulses of magmatic activity (see below).

The structural setting of basaltoid magmatism has long been discussed by several geologists, starting with D. I. Mushketov [*Mouchketoff*, 1928], who tried to correlate magmatic pulses with orogenesis in the Pyrenees. Later it was hypothesized [*Mallarach and Riera*, 1981; *Marti et al.*, 1992] that the volcanic centers are spatially constrained to northwest- and northeast-trending fault zones, which predetermined and controlled the development of the rift depressions. However, the basalt fields seem not to show any systematic relations with these depressions: the thicknesses of the Neogene-Quaternary rocks do not exceed a few dozen meters [*Losantos et al.*, 1989], neither were any seismic activity detected in the area [*Gallart et al.*, 1984], and hence, there are no sufficient reasons to recognize these rifts. It is also worth mentioning that attempts to relate any manifestations of magmatic activity in this part of Spain with the development of the Valencia trough near the Iberian margin [*Marti et al.*, 1992] seem to be groundless, because this trough developed as a rift basin until the mid-Miocene, after which a post-rifting episode of passive thermal subsidence began [*Catalan and Davila*, 2001].

Similar to several other areas of intraplate basaltoid volcanism (such as Mongolia, the Vitim Plateau in south-central Siberia, Massif Central in France, Bohemian Massifs, etc.), this territory is classed with regions of pre-rifting tectonic regime with typical combinations of low-thickness sedimentary rocks of the platform type and products of fissure eruptions [*Grachev*, 2000; *Grachev and Devyatkin*, 1997; *Grachev et al.*, 1981]. We believe that this exactly tectonic regime is typical of the modern geodynamics in the area discussed herein.

Basaltoid volcanism in this part of Catalonia was studied for a long enough time. The common features of the basalt landforms and local cinder cones are described (together with data on the chemistry of the volcanics) in numerous publications [*Arana et al.*, 1983; *Coy-Yll et al.*, 1974; *Lopez Ruiz et al.*, 1985; *Mallarach and Riera*, 1981; *Marti et al.*, 1992; *Montoto and Esbert*, 1967; *Tournon*, 1968], but the very first isotopic-geochemical data that make it possible to estimate the probable composition of the mantle sources were not obtained until very recently [*Cebria et al.*, 2000; *Neumann et al.*, 1999].

The slag-lava composing the Roca Negra volcano contains abundant xenoliths of biotite and amphibole pyroxenite, amphibolite, and gabbro. The first data on the bulk-rock composition of the xenoliths and the chemistry of their minerals were presented in [*Ancochea and Nixon*, 1987; *Llobera Sanchez*, 1983; *Tournon*, 1968]. Pioneering data on the composition of xenoliths of the Roca Negra volcano (pyroxenite, amphibolite, and gabbro) in [*Llobera Sanchez*, 1983] were used by this author to calculate the crystallization temperatures and pressures of these rocks in the upper mantle: 1000–1100°C and approximately 10 kbar; and later similar estimates were published in [*Neumann et al.*, 1999].

We used a representative collection of the mantle xenoliths to obtain new data on their whole-rock composition, concentrations of trace elements, and their Sr, Nd, and He isotopic composition, as well on their age.

[1]Institute of Physics of the Earth, Russian Academy of Sciences, Moscow, Russia

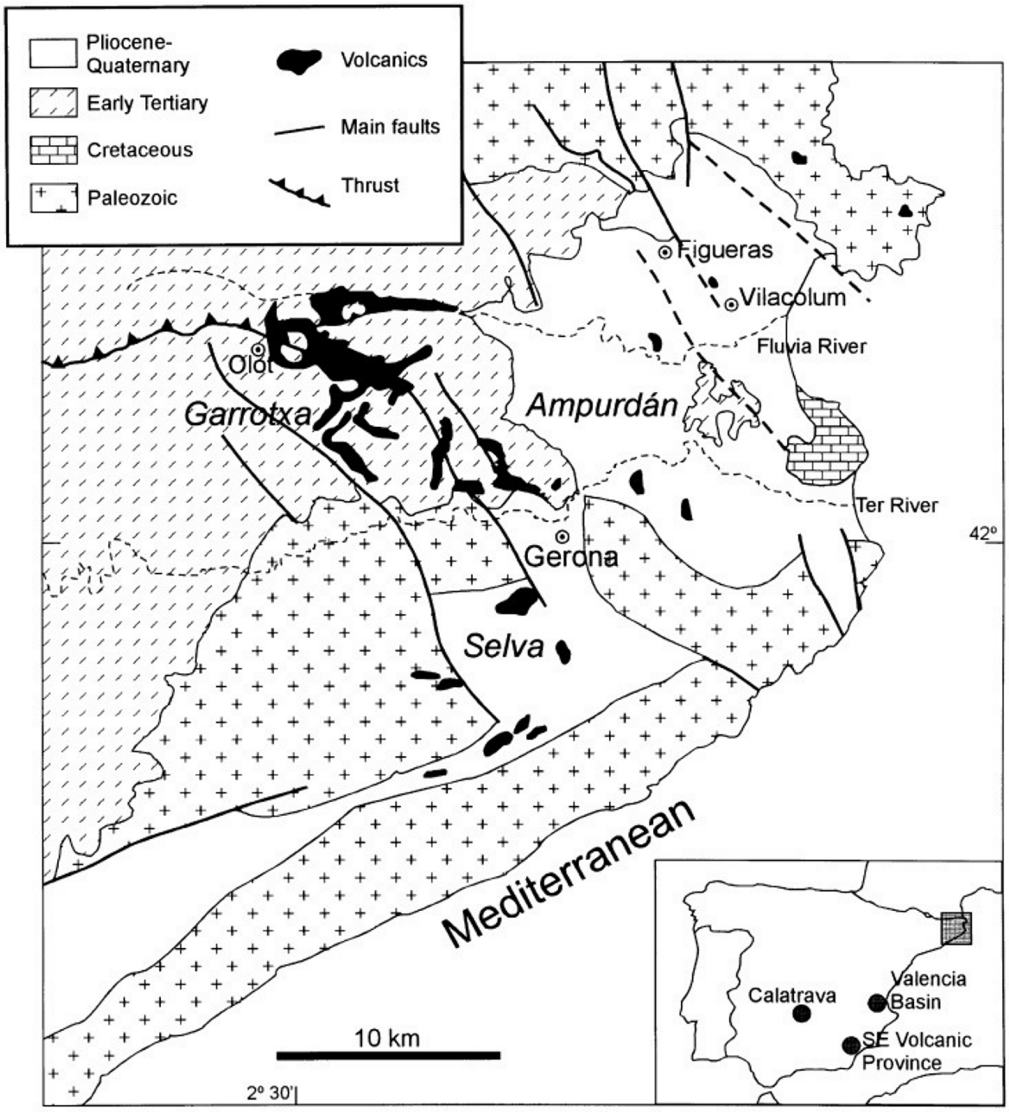

Figure 1. Geological map of the volcanic region in NE Spain. The inset shows the location of the other Neogene-Quaternary volcanic areas in Spain [*Cebria et al.*, 2000].

Methods

Analyses for trace and rare-earth elements were carried out at the Laboratory of Nuclear Physical Methods at the Experimental and Test Expedition of GGP Sevzapgeologiya (St.-Petersburg) (ETE GGP Sevzapgeologiya) by instrumental neutron activation analysis (INAA) and X-ray fluorescence spectroscopy (XRF). In the INAA measurements, 150–250 mg batches of the material packed into hermetically sealed ultrapure quartz capsules were irradiated in the test channel of the thermal column of the WWR-M reactor at the Nuclear Physics Institute in Gatchina. The exposure time was 10 hours with a thermal neutron flux of 7.5×10^{13} n/cm^2 s. For metrological provision, USGS reference materials (AGV-2, G-2, W-2, BIR-1, BHVO-1) were used, which were made available for us by courtesy Dr. Miller. The reference materials were irradiated in the same cell with the tested specimens. The measurements were carried out in three steps with a quenching time of 6, 12, and 35 days, respectively.

X-ray fluorescence analysis followed the original experimental procedure developed in the ETE GGP Sevzapgeologiya and certified by the Scientific Council on Analytical Methods, All-Russia Institute of Mineral Resources, in 1989. The 20-g batches of samples ground to 200 mesh were packed into a special tray. The characteristic radiation was excited by (a) an X-ray tube with an intermediate silver target and (b) an Am-241 radioactive isotope source. For metrological provision of XRF measurements, we used the BM, SGD-1A, SG-1A, ST-1A, SA-1, TB, and SGXM-3 reference samples.

Extraction of monomineral fractions from the deep xenoliths was carried out by sample crushing in heavy liquids and subsequent electromagnetic separation of the minerals.

Table 1. Modal Composition (%) of Xenoliths in Basalts of the Roca Negra Volcano

	Ol	Cpx	Opx	Amph	Mica	Plag	Ox	Apat	Glass	Pores
RC-1x	2	48	-	-	47	-	1	-	2	-
RC-2x	-	40	-	30	-	10	17	-	-	3
RC-4x	4	-	12	16	5	61	2	-	-	-
RC-5x	-	50	-	34	-	-	8	traces	7	2
RC-7x	2	10	-	34	-	-	15	-	35	4
RC-8x	-	65	-	-	-	20	3	-	10	2
RC-9x	-	45	-	-	49	-	3	2	-	-
RC-11	3	45	-	37	5	3	7	-	-	-
RC-10	1	5	-	5	87	-	2	-	-	-
RC-10/1	1	4	-	91	0.5	1	1	1	-	-

When necessary, the concentrates were subjected to the additional manual purification to reach a purity of the fractions of 95–99%.

Extraction of helium was carried out by melting for the whole-rock samples [*Kamensky et al.*, 1990] and by crusting up to monomineral fractions [*Ikorskii and Kamensky*, 1998) at the Laboratory of Geochronology and Geochemistry of Isotopes at the Geological Institute of the Kola Research Centre, Russian Academy of Sciences. The crushing method is suitable for selective extraction of gases from fluid inclusions, which reduces the effects of radioactive gases accumulated in the volume of the crystalline cell of the minerals [*Kaneoka et al.*, 1978). When extracting the gases, the specimens with a weight of 0.16–2.25 g, together with the milling steel rollers, were placed into a glass crucible, which was then evacuated and sealed. Milling was achieved by the vibration of the crucible.

The isotopic composition and He concentration were measured by the MI-1201 mass spectrometer no. 22-78 with a sensitivity to helium of 5×10^{-5} A/torr. The concentrations are measured by the peak height method with an error of 5% ($\pm 1\sigma$); the errors of the isotopic ratios were $\pm 20\%$ at $^3He/^4He = n \times 10^{-8}$ and $\pm 2\%$ at $^3He/^4He = n \times 10^{-6}$. The blank tests were carried out after recharging of the cartridge in the same conditions as the analyses of the samples. The isotopic composition of Sm and Nd were measured by a Finnigan MAT-261 mass spectrometer at the Geological Institute of the Kola Research Center, Russian Academy of Sciences. The extraction of Sm, Nd, Rb, and Sr followed the procedure suggested in [*Richards et al.*, 1976). The measurement errors for the isotopic composition of Nd do not exceed 0.005%, and the errors in the determination of Sm/Nd are no higher than 0.3. The isotopic composition of Nd is corrected against the La Jolla standard value $^{143}Nd/^{144}Nd = 0.511860$; the value of $^{148}Nd/^{144}Nd = 0.241570$ is used as the normalizing factor. For uranium concentration radiographs for fragments of uranium fission were obtained during irradiation of petrographic thin sections by heat neutrons from a nuclear reactor [*Grachev, Komarov*, 1994). The flow of neutrons was $(2 - 8) \times 10^{15}$ N/cm^2. Microsections were prepared on slides of radiation-resistant quartz glass with an application of epoxy glass. Synthetic mica was used as a detector. All auxiliary materials (glass, mica, diamond abrasive) had low uranium concentration ($< 5 \times 10^{-10}$ g/g). Special attention was paid to the cleaning of micro sections after polishing. The uranium content was determined by a calculation of tracks of the splinters of uranium fission, fixed on the radiographs of the minerals or the entire micro section. The standards BCR and PCC of uranium were used for comparison. Accuracy of uranium content measurements depended on the number of counted tracks. For the concentration $n \times 10^{-9}$ g/g this accuracy was 20–25%, while for $n \times 10^{-9}$ and higher it was 10% and less.

Modal and Chemical Composition of the Xenoliths

Our xenolith samples show their well preserved original ellipsoidal morphologies, and their sizes are up to 15–20 cm along their major axes and up to 6–8 cm along minor axes (Figure 2). The contacts between the xenoliths and host rocks are sharp, with obvious traces of chilling within thin (no thicker than 1–2 mm) zones. The slag-lavas abound in xenoliths of biotite and amphibole pyroxenite, amphibolite, and gabbro, with pyroxenite and amphibolite being dominant and gabbro found merely as occasional fragments.

The modal composition of the xenoliths broadly varies (Table 1), and their following lithologies can be distinguished: hornblende pyroxenite, mica pyroxenite, amphibolite, glimmerite, and gabbro. As can be see in thin sections, the rocks show broad variations in both the compositions of their minerals and their sizes and mutual relations.

The hornblende pyroxenite is a hypidiomorphic-granular or allotriomorphic-granular rock with large (up to 3.5 mm) grains of clinopyroxene, which are often replaced by pistachio-colored hornblende in the margins. The grains of the latter mineral are smaller and anhedral. As is also often seen in thin sections, both minerals quite often contain poikilitic inclusions of an ore mineral, and the rock then acquires a sideronitic to poikilitic texture.

The micaceous pyroxenite has the same texture as the hornblende pyroxenite and contains anhedral dark-orange biotite and greenish pyroxene grains (seen under an opti-

=

Table 2. Chemical Composition (wt %) of Xenoliths in Basalts From the Roca Negra Volcano and Neighboring Areas

Component	RC-1x 1	RC-2x 2	RC-4x 3	RC-5x 4	RC-7x 5	RC-8x 6	RC-9x 7	RC-10/1x 8	RC-10/2x 9	RC-10/3 10	RC-11x 11	RC-1/5 12	RC-1/11 13	RC-1/6 14	CAADR 15	RN-25 16	RN-36 17
SiO_2	45.02	37.98	46.12	35.66	38.86	45.88	39.42	40.54	44.27	40.14	45.18	33.79	41.73	44.97	44.28	38.59	43.35
TiO_2	1.34	3.58	0.30	3.50	3.90	1.86	2.96	4.00	2.74	2.15	1.76	4.69	2.50	0.05	0.15	2.81	2.94
Al_2O_3	6.51	11.82	21.19	9.56	13.98	12.16	12.07	13.75	16.03	8.47	7.33	9.89	10.21	1.22	4.09	15.56	11.47
FeO*	10.42	19.10	7.41	23.93	13.65	10.49	14.61	13.41	14.66	14.41	10.56	22.85	15.18	7.49	9.14	15.90	14.53
MnO	0.25	0.25	0.14	0.25	0.15	0.21	0.41	0.18	0.17	0.34	0.19	0.19	0.16	0.13	0.13	0.10	0.07
MgO	18.24	9.92	11.29	9.27	11.29	11.75	13.05	11.62	7.58	13.30	14.32	9.99	14.68	43.71	38.59	11.05	12.57
CaO	13.62	14.16	11.62	14.34	12.68	14.34	10.53	12.53	10.77	13.37	17.81	14.59	14.17	1.41	3.17	12.09	13.05
Na_2O	0.82	1.37	0.96	0.88	1.69	1.48	1.48	2.14	2.27	1.66	1.11	1.47	0.88	0.36	0.36	2.00	1.72
K_2O	2.47	0.61	0.33	0.28	1.44	0.36	2.89	0.98	0.68	1.39	0.39	0.40	0.21	0.02	0.03	1.15	0.41
P_2O_5	0.13	0.16	0.11	0.17	0.17	0.13	0.92	0.16	0.17	0.05	0.12	0.19	0.11	-	0.03	0.25	0.13
Cr_2O_3	0.024	0.062	0.042	0.060	0.21	0.20	0.06	0.014	0.04	0.03	0.13	0.01	-	0.46	-	0.08	-
NiO	0.012	0.006	0.002	.0045	0.0082	0.013	0.016	0.010	0.06	0.01	0.01	-	-	-	-	-	-
V_2O_5	0.006	0.078	0.020	0.060	0.036	.0074	0.074	0.052	0.07	0.05	0.052	-	-	-	-	-	-
SO_3	0.045	0.036	0.009	0.39	0.15	0.058	0.12	0.027	0.38	0.02	0.045	-	-	-	-	-	-
CO_2	0.01	0.18	0.07	0.32	0.01	0.11	0.04	0.04	0.03	0.03	0.32	-	-	-	-	-	-
H_2O	0.19	0.25	0.01	0.86	0.62	0.44	0.23	0.12	0.12	1.11	0.39	-	-	-	-	0.31	0.47
LOI	0.83	0.75	0.29	1.96	1.79	0.87	1.32	0.37	0.39	2.37	0.92	0.89	-	-	-	-	-
Total	99.65	99.70	99.76	99.80	99.60	99.63	99.66	99.33	100.43	98.90	99.69	98.95	99.83	99.82	99.97	99.89	100.71
Or	5.47	3.60	1.95	1.65	2.22	13.28	6.19	5.67	4.02	-	2.30	-	1.24	0.12	0.18	-	2.43
Ab	-	1.20	8.12	0.34	-	-	-	3.37	19.21	-	2.13	-	7.02	2.54	3.05	-	8.09
An	6.79	24.30	52.54	21.31	26.31	18.00	17.76	25.08	31.54	11.55	14.00	19.21	23.29	1.92	9.46	30.08	22.37
Lc	7.16	-	-	-	4.93	2.98	8.54	-	-	6.44	-	1.85	-	-		5.33	-
Ne	3.76	5.63	-	3.85	7.75	6.78	6.78	7.98	-	7.61	3.94	6.74	0.23	-	-	9.17	3.50
Hy	-	-	17.24	-	-	-	-	-	0.40	-	-	-	-	23.93	18.16	-	-
Di	46.65	34.95	3.51	38.51	27.69	37.21	37.21	28.05	16.86	37.00	57.27	30.87	36.03	3.96	4.77	20.16	29.02
Ol	16.69	5.96	12.45	6.07	11.18	11.34	11.34	11.17	14.96	19.36	6.39	7.41	13.92	61.53	59.45	19.33	19.30
Cs	-	-	-	-	-	-	-	-	-	2.57	-	3.80	-	-	-	0.96	-
Mt	8.28	-	2.84	19.07	9.93	6.71	6.71	-	6.76	6.39	6.48	12.78	7.68	5.21	4.55	8.55	11.42
Hm	1.19	16.29	-	-	-	-	-	12.24	-	-	2.69	6.05	5.11	-	-	-	-
Il	2.45	6.47	0.57	6.65	7.41	3.53	5.62	2.86	5.20	4.08	3.34	8.91	4.75	0.09	0.28	5.34	4.60
Ap	0.31	0.38	0.26	0.40	0.40	2.18	2.18	0.38	0.40	0.12	0.28	0.45	nd	nd	0.07	0.59	0.56

Note: 1–13 – xenoliths from the Roca Negra volcano (author's data), 14 – spinel lherzolite xenolith in basalt from Puig de Banya de Boc volcano (author's data), same, Gerona area [*Coy-Yll et al.*, 1974], 16, 17 – xenoliths from the Roca Negra [*Tournon*, 1968].

Figure 2. Sample of micaceous pyroxenite with clearly seen shiny mica flakes (49%) in a dark mass of clinopyroxene (50%). Scale: one penny coin.

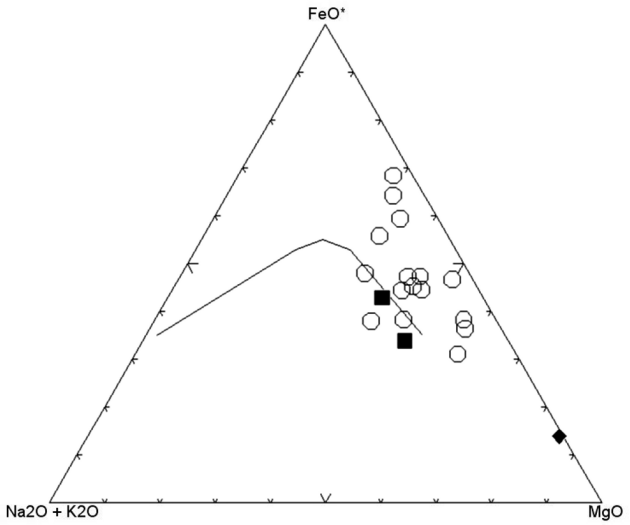

Figure 3. AFM diagram for xenoliths (open circles) and host basalts (solid circles) from the Roca Negra volcano.

cal microscope). The biotite platelets are larger than the pyroxene grains, and the boundaries between grains of these minerals are not linear, with mutual embayment.

The amphibolite, which sometimes contains as much as 90% hornblende, has a panidiomorphic-granular texture. The gabbro contains up to 70% plagioclase, up to 15% orthopyroxene, and up to 5% hornblende.

We failed to find spinel lherzolite or pure pyroxenite xenoliths in the rocks of the volcano, which does not, however, mean that these rock do not contain such xenoliths at all, because spinel lherzolite xenoliths are often found in the lavas of nearby volcanoes, for example, Puig de Banya de Boc volcano [*Oliveras and Galán*, 2006), but only occasionally contain pyroxenite xenoliths and do not contain amphibolite xenoliths at all.

The whole-rock composition of xenoliths from the Roca Negra volcano shows broad variations in the concentrations of major components (Table 2), which is understandable with regard for the variations in the modal composition of the rocks (Table 1). The AFM diagram (Figure 3) displays a well pronounced Fenner differentiation trend: the composition points of the xenoliths lie along the $FeO_t - MgO$ line. This is confirmed by results of factor analysis (method of main components) of the major-component composition of the xenoliths (Table 3): the contribution of Factor 1 $Mg_{92}/Ti_{88}Na_{79}Ca_{76}Fe_{72}$ to the overall variability of the rocks is 46.4%. As also follows from Figure 3, which also shows the composition of a spinel lherzolite xenolith from Puig de Banya de Boc volcano (solid diamond), the lherzolite and pyroxenite do not compose a continuous compositional series, and the compositional gap between them may be indicative that these rocks are not genetically interrelated.

Table 3. Matrix of the Factor Loadings of Major Components

Component	Factor 1	Factor 2
SiO_2	-0.68	-0.48
TiO_2	**0.89**	0.31
Al_2O_3	0.59	-0.10
FeO	**0.72**	0.48
MnO	0.39	-0.54
MgO	**-0.92**	0.02
CaO	**0.76**	0.01
Na_2O	**0.79**	-0.04
K_2O	0.37	**-0.86**
P_2O_5	0.39	**-0.81**
Input (%) to total variability	46.4	22.6

Note: significant loadings are printed in bold type.

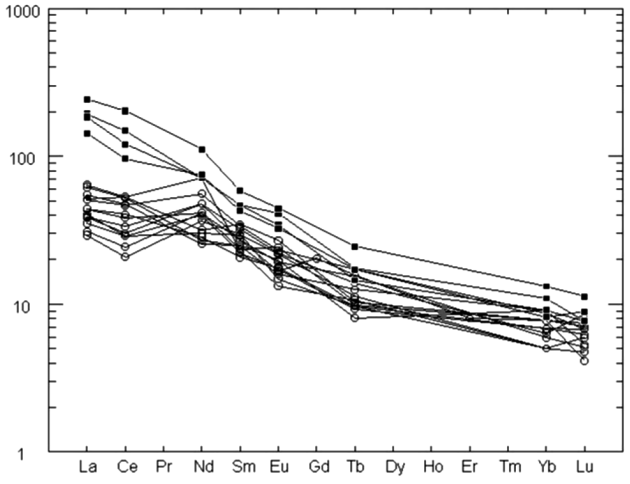

Figure 4. Chondrite-normalized [*McDonough and Sun*, 1995) REE patterns.

Table 4. REE Concentrations (ppm) of Xenoliths Hosted by Basalts From the Roca Negra Volcano

Element	RC-1x	RC-2x	RC-3x	RC-4x	RC-5x	RC-6x	RC-8x	RC-9x	RC-10/2x	RC-10/3x	RC-1/5	RC-1/11	RC-11
La	16.70	21.10	16.60	12.60	11.60	14.50	9.60	13.30	14.40	18.10	12.80	10.20	20.30
Ce	46.00	46.00	40.40	29.00	25.00	35.00	18.00	25.00	33.00	41.00	26.00	21.00	45.00
Nd	45.00	20.00	35.00	30.00	19.00	18.00	23.00	25.00	18.00	19.00	30.00	26.00	17.00
Sm	4.60	7.00	6.80	6.50	5.90	4.20	6.00	4.50	4.80	5.10	5.50	5.50	5.00
Eu	1.02	2.07	1.77	1.71	1.68	1.35	1.14	1.32	1.85	1.52	1.48	1.29	1.23
Tb	0.53	0.51	0.85	0.69	0.56	0.48	0.48	0.46	0.49	0.40	0.77	0.78	0.62
Yb	1.10	1.70	1.90	1.40	1.10	1.50	1.10	1.50	1.70	2.00	1.30	1.70	2.00
Lu	0.20	0.24	0.23	0.29	0.20	0.23	0.16	0.21	0.14	0.18	0.17	0.25	0.18

The REE patterns of the xenoliths and their host basalts show variable enrichment in LREE (Table 4, Figure 4).

Uranium concentrations in our bulk-rock xenolith samples range from 32 to 370×10^{-3} ppm and reach $13,500 \times 10^{-3}$ ppm in apatite in recrystallized domains (Table 5).

Table 5. Uranium Concentrations (10^{-3} ppm) in Xenoliths From the Roca Negra Volcano

Sample	Rock	Opx	Bt	Amph	Ap	Whole-rock sample
RC88-1/5	pyroxenite	-	-	-	-	370
RC88-1x	pyroxenite	31	10	-	-	32
RC88-1/11	pyroxenite	36	61	107	13500	125
RC88-4x	gabbro	-	-	-	-	160
RC88-1/6	lherzolite	-	-	-	-	110

Mineral Chemistry

The major rock-forming minerals are clinopyroxene (diopside), hornblende (kaersutite), mica (biotite and phlogopite), plagioclase (labradorite), spinel, ilmenite, more rare olivine (forsterite) and orthopyroxene (bronzite), and apatite as inclusions in clinopyroxene and amphibole.

Phlogopite is a mineral of greatest interest for understanding the nature of the xenoliths. Its contents in the rocks vary from 5 to 87% (Table 6), which is a fairly rare phenomenon and is usually thought to be an indication of intense metasomatism. The mica occurs as prismatic crystals that are in textural equilibrium with other minerals. The phlogopite shows remarkable variations in the Ti concentrations (from 0.5 to 4 wt %) at a Mg concentration of 16 to 20 wt % (Figure 5). In contrast to rocks of the MARID suite,

Table 6. Chemical Composition (wt %) of Micas in Xenoliths From the Roca Negra Volcano in Comparison With Composition of Micas in Other Ultramafic Rocks

Component	1	2	3	4	5	6	7	8	9	10	11	12	13	14
SiO_2	35.46	37.07	37.33	36.62	37.41	37.53	36.94	37.87	36.57	38.97	38.91	37.68	39.98	41.0–42.7
TiO_2	5.45	2.30	4.77	1.20	5.91	6.23	2.70	2.66	9.20	2.86	3.67	5.53	9.13	1.07–1.59
Al_2O_3	16.58	17.46	16.12	17.30	16.74	16.76	17.03	16.40	15.84	13.80	14.62	16.18	13.45	11.7–13.2
Cr_2O_3	0.19	0.05	0.60	0.32	0.19	0.35	0.07	0.70	–	0.15	0.17	0.43	0.71	0.19–0.81
FeO*	15.35	11.78	14.30	10.91	6.91	6.71	8.32	5.46	12.82	8.18	9.88	9.72	3.57	2.72–4.57
MnO	0.03	0.12	0.50	0.13	0.07	0.05	0.10	0.02	–	0.04	0.05	0.01	0.04	0.0–0.5
MgO	13.64	17.82	15.66	19.78	18.40	18.41	19.62	21.96	12.87	19.44	17.72	17.53	18.73	23.9–25.5
CaO	0.13	0.00	0.00	0.00	0.03	0.05	0.11	0.07	–	–	0.07	0.04	–	0.05
Na_2O	1.30	1.97	0.94	2.34	0.56	0.61	0.46	0.13	1.11	0.49	0.30	0.52	0.06	0.17–0.43
K_2O	8.72	8.48	8.56	9.53	9.83	9.73	10.05	10.32	8.92	9.51	9.83	9.46	9.64	9.27–9.97

Note: the Roca Negra: 1 – average biotite composition (9 analyses); 2 – average phlogopite composition (4 analyses); 3, 4 – phlogopite [*Sanchez*, 1983], 5–7 – central Spain, 5 – average phlogopite composition in glimmerites (10 analyses), 6 – average phlogopite composition in spinel lherzolites (5 analyses), [*Ancochea and Nixon*, 1987], 7, 8 – phlogopite in phlogopite pyroxenite xenoliths from Roccamonfina volcano, Italy (7 and 5 analyses) [*Giannetti and Luhr*, 1990], 9 – phlogopite in spinel lherzolite xenolith in basalts at the Bartoi River, Baikal Rift, Russia [*Ionov and Hofmann*, 1995], 10 – phlogopite in glimmerite in peridotite from the Bohemian Massif [*Becker et al.*, 1999], 11 – phlogopite in xenolith form the Roberts Victor kimberlite pipe [*MacGregor*, 1979], 12 – xenolith of micaceous websterite [*Lasko and Sharkov*, 1988], 13 – garnet peridotite, Tanzania [*Dawson*, 1972], 14 – variations in mica composition in metasomatic zones in peridotites [*Dawson and Smith*, 1977].

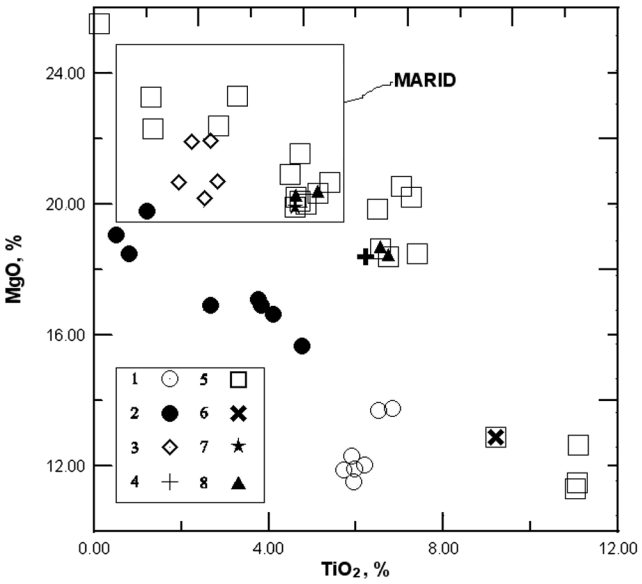

Figure 5. MgO – TiO_2 diagram for mica in xenoliths from the Roca Negra volcano in comparison with mica compositions in xenoliths collected elsewhere. 1, 2 – Biotite and phlogopite, the Roca Negra volcano; 3 – phlogopite in phlogopite pyroxenite xenoliths, Roccamonfina [*Gianetti and Luhr*, 1990]; 4 – average composition of phlogopite in spinel lherzolites [*Ancochea and Nixon*, 1987]; 5 – phlogopite in spinel lherzolite xenoliths hosted by basalts in the Baikal rift and Mongolia [*Ionov and Hofmann*, 1995]; 6 – garnet peridotite, Tanzania [*Dawson*, 1972], 7 – phlogopite in xenolith from the Roberts Victor kimberlite pipe [*MacGregor*, 1979]; 8 – phlogopite in xenoliths form the Premier Mine pipe, South Africa [*Danchin*, 1979]. The rectangle outlines the composition field of phlogopite in xenoliths of the MARID suite [*Dawson and Smith*, 1977].

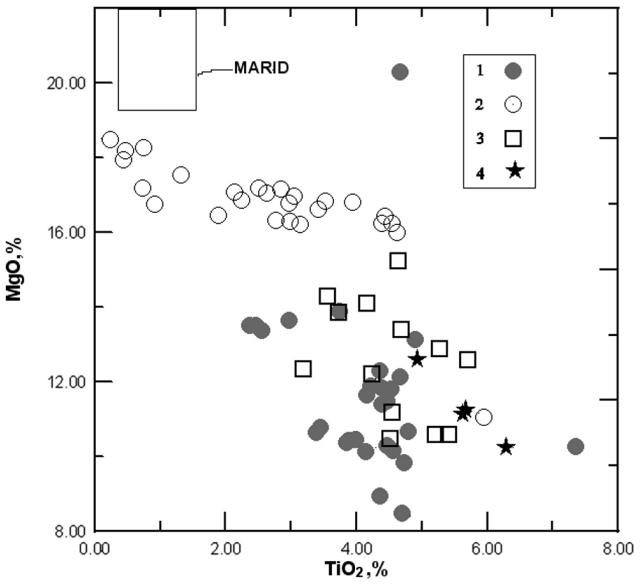

Figure 6. MgO – TiO_2 diagram for amphibole in xenoliths from the Roca Negra volcano in comparison with mica compositions in xenoliths collected elsewhere. 1 – Amphibole in xenoliths from the Roca Negra volcano; 2 – amphibole in spinel lherzolite xenoliths from the Baikal rift, Rhine graben, and Mongolia [*Ionov and Hofmann*, 1995; *Ionov et al.*, 1984; *Witt and Seck*, 1989]; 3 – amphibole in pyroxenite xenoliths from the canary Islands, Frank Seamount in the Indian Ocean, the Cape Verde Islands in the Atlantic Ocean, Murcia, and the Tien Shan [*Kogarko*, 1990; *Munoz et al.*, 1974; *Reid and Le Roex*, 1988; *Sagredo*, 1969]; 4 – amphibole in pyroxenite xenoliths from the Tien Shan [*Dobretsov and Dobretsova*, 1975]. The rectangle contours the amphibole composition field in xenoliths of the MARID suite [*Dawson and Smith*, 1977].

phlogopite in the Roca Negra xenoliths bears high total Fe concentrations (11–16 wt %) and lower Mg concentrations (Figure 5). Based on its TiO_2 concentrations, phlogopite in the Roca Negra xenoliths can be classified into two groups: with $>$ 2 wt % and $<$ 2 wt % TiO_2. As can be seen in Figure 5, the low-Ti phlogopite varieties are closely similar to phlogopite in the MARID suite and xenoliths in ultrapotassic lava of Roccamonfina and Torre Alfina volcanoes [*Conticelli*, 1998; *Gianetti and Luhr*, 1990].

Amphibole was found in most of the xenoliths, both phlogopite-bearing and phlogopite-free (Table 7). The mineral usually occurs in embayments between olivine and clinopyroxene or as inclusions in clinopyroxene. The amphibole was first classed with pargasite-ferrohastingsite [*Tournon*, 1968] based on a single analysis of the mineral, but its high TiO_2 concentration (Table 7) provides a ground to attribute the amphibole of the Roca Negra xenoliths to kaersutite. As can be seen in Figure 6, this amphibole is compositionally identical with amphibole in xenoliths in oceanic-island basalts [*Frisch and Schminke*, 1970; *Kogarko*, 1990; *Munoz et al.*, 1974; *Reid and Le Roex*, 1988; *Sagredo*, 1969] and such intraplate magmatic areas as the Tien Shan [*Dobretsov and Dobretsova*, 1975].

The amphibole is different from amphibole in spinel lherzolites, but the insignificant gap in the MgO concentration (Figure 6) seems to be explained by an insufficient number of analyses, whose greater number shall likely bridge this gap.

Finally, it is important for the further discussion that phlogopite pyroxenite xenoliths from Roccamonfina volcano [*Gianetti and Luhr*, 1990] and phlogopite-bearing xenoliths of Torre Alfina volcano [*Conticelli*, 1998] do not contain amphibole (more specifically, it still has not been found in these rocks). Note that the lavas hosting these xenoliths are ultrapotassic, in contrast to the sodic basalts of the Roca Negra volcano.

The distribution of phlogopite and amphibole in xenoliths shows their certain antagonism, and these minerals were found together only in rare instances (for example, in Kazakhstan and the Tien Shan) and only in xenoliths showing no unambiguous evidence of their mantle provenance [*Dobretsov et al.*, 1975, p. 208]. However, as was demonstrated above (Table 6 and Table 7), detailed data on xenoliths in lavas within continental and/or oceanic lithospheric domains indicate that both minerals are related in a paragenetic manner and can occur together in garnet and spinel lherzolites, whose mantle provenance does not provoke any doubt [*Boyd*

Table 7. Average Chemical Composition (wt %) of Amphiboles in Xenoliths From the Roca Negra Volcano in Comparison With Amphibole Compositions in Other Rocks

Component	1	2	3	4	5	6	7	8	9	10	11	12	13
SiO_2	38.46	39.92	40.10	38.65	42.57	39.85	41.15	40.89	42.21	42.92	43.90	43.76	39.77
TiO_2	4.58	3.78	4.33	2.97	4.79	7.35	4.14	5.64	1.02	2.62	3.52	2.97	5.67
Al_2O_3	13.50	14.54	13.03	16.61	11.05	12.69	14.61	14.25	15.15	14.56	13.63	14.05	14.06
FeO*	16.29	13.99	14.08	13.08	10.38	9.50	8.05	6.23	4.33	3.40	3.81	4.02	11.25
MnO	0.35	0.00	0.00	0.07	0.45	0.43	0.05	0.09	0.07	0.04	0.05	0.07	0.12
MgO	9.66	10.47	11.65	13.65	10.66	10.27	14.46	14.97	17.34	17.04	16.85	16.79	11.47
CaO	10.76	11.87	10.71	11.05	12.63	13.03	11.42	11.35	11.62	10.96	10.82	10.56	10.64
Na_2O	3.17	3.15	2.92	2.44	2.97	2.63	2.36	2.15	3.32	3.31	3.85	3.49	2.74
K_2O	1.32	0.32	1.08	1.26	0.84	0.83	2.17	2.13	0.06	1.63	0.67	1.35	1.40
Cr_2O_3	-	0.26	-	-	-	-	0.17	0.89	0.82	1.06	0.86	0.18	-
N	6	6	5	1	1	1	3	2	3	1	1	1	2

Note: the Roca Negra: 1 – sample RC1/10, 2 – sample RC1/5, 3 – sample RC10/3 (this publication), 4 – amphibole [*Tournon*, 1968], 5, 6 – sample 15126: 5 – grain core, 6 – grain margin [*Sanchez*, 1983], 7–9 – central Spain: 7 – K–Ti pargasite in glimmerite, 8 – K-kaersutite in micaceous lherzolite, 9 – pargasite in spinel lherzolite [*Ancochea and Nixon*, 1987], 10–11 – spinel lherzolite xenoliths [*Ionov et al.*, 1984], 12 – pargasite in lherzolite xenolith [*Dawson and Smith*, 1977], 13 – kaersutite in xenoliths in basalts from the Tien Shan [*Dobretsov and Dobretsova*, 1975].

Table 8. Chemical Composition (wt %) of Clinopyroxene in Xenoliths From the Roca Negra Volcano

Component	1	2	3	4	5	6	7	8	9	10	11	12	13	14
SiO_2	52.96	52.85	52.93	44.89	45.94	47.11	46.21	42.09	43.14	45.52	45.46	46.30	45.36	46.23
TiO_2	0.44	-	-	2.91	2.22	2.24	2.33	3.94	3.14	2.27	2.26	2.37	2.47	2.41
Al_2O_3	3.07	2.88	2.93	10.63	8.66	7.76	8.62	14.01	13.57	9.39	8.77	8.28	8.39	8.62
Cr_2O_3	1.13	1.49	1.18	-	0.24	-	-	-	-	-	-	-	-	-
FeO*	2.27	2.77	2.42	8.75	8.75	7.59	8.19	11.13	10.84	8.86	9.60	9.00	9.40	8.74
MnO	-	-	0.39	-	-	0.28	-	-	-	-	-	-	-	-
MgO	18.22	18.05	18.06	10.63	10.66	11.48	11.18	11.53	11.32	12.25	12.06	11.90	12.12	12.40
CaO	21.40	21.12	21.36	21.07	22.68	22.29	22.45	14.79	15.60	20.54	21.10	21.13	21.44	20.78
Na_2O	0.55	0.83	0.72	1.11	0.85	1.25	1.02	2.51	2.25	1.12	0.70	0.95	0.79	0.77
Wo	44.20	43.85	44.05	49.69	51.51	50.59	50.96	38.06	39.78	46.64	46.92	47.62	47.45	46.64
En	52.33	52.10	51.80	34.87	33.67	36.24	35.30	41.27	40.14	38.69	37.30	37.30	37.31	38.71
Fs	3.48	4.06	4.14	15.44	14.82	13.17	13.75	20.66	20.08	14.67	15.78	15.07	15.24	14.65
	15	16	17	18	19	20	21	22	23	24	25	26	27	28
SiO_2	48.21	48.90	48.73	49.02	49.33	47.18	47.49	47.23	45.44	46.68	46.75	47.41	47.30	47.13
TiO_2	1.33	1.22	1.38	1.03	1.02	2.46	2.43	2.31	2.85	2.59	1.96	2.27	1.62	1.86
Al_2O_3	6.60	6.52	6.77	6.27	5.94	6.11	5.68	5.97	6.93	7.08	7.29	6.96	7.27	6.87
Cr_2O_3	-	-	-	0.30	-	-	-	-	-	-	-	-	-	-
FeO*	8.27	7.55	7.49	7.99	8.30	8.55	7.48	7.59	8.79	7.33	10.11	9.39	9.63	9.62
MnO	0.39	0.31	0.38	-	-	-	0.63	0.27	-	-	-	-	0.25	0.28
MgO	14.22	14.77	14.49	14.44	14.47	13.13	14.01	14.76	13.20	13.28	11.13	11.12	11.48	11.50
CaO	20.14	20.34	20.07	20.02	20.29	22.24	22.29	21.42	22.21	22.76	20.77	21.04	20.79	21.16
Na_2O	0.83	0.40	0.70	0.92	0.65	-	-	0.44	0.57	-	1.71	1.80	1.65	1.57
Wo	43.49	43.44	43.52	43.51	43.50	47.29	46.54	44.92	47.34	48.44	47.42	48.50	47.30	47.71
En	42.72	43.88	43.70	43.65	43.15	38.83	40.68	43.05	39.31	39.31	35.34	35.65	36.33	36.06
Fs	13.78	12.68	12.79	12.85	13.34	13.87	12.78	12.03	12.25	12.25	17.24	15.85	16.37	16.23

Table 9. Chemical Composition (wt %) of Titanomagnetite in Xenoliths From the Roca Negra Volcano

Component	1	2	3	4	5	6	7	8	9	10
SiO_2	0.39	0.50	0.70	0.41	0.38	-	0.57	-	0.44	0.39
TiO_2	9.81	6.42	7.58	7.46	21.28	2.92	2.80	0.66	1.06	1.76
Al_2O_3	6.80	6.89	6.86	6.86	12.45	10.71	6.29	21.55	22.13	8.99
FeO*	77.95	78.83	80.39	81.11	58.99	80.27	86.40	68.14	67.42	84.76
MnO	-	-	-	-	-	0.61	-	0.53	-	-
MgO	4.64	5.22	4.13	4.07	5.78	5.15	3.57	8.20	8.67	4.34
Cr_2O_3	-	-	-	-	0.88	0.83	-	-	-	-

and Meyer, 1979; *Melyakhovetskii et al.*, 1988; *Zharikov and Grachev*, 1987; and others], and in pyroxenite and amphibolite xenoliths of various composition in lavas of various composition. Considering that both phlogopite and amphibole are indicators of the fluid regime in the Earth's interiors, one of the possible means of solving the problem is to elucidate the circumstances at which melts are derived in which amphibole and phlogopite are antagonists, as in the lavas of Roccamonfina and Torre Alfina volcanoes [*Conticelli*, 1998; *Gianetti and Luhr*, 1990].

Olivine was found only in a few of the xenoliths and is often accompanied by amphibole and clinopyroxene. The composition of the olivine varies from 78 to 82% of the forsterite end member at an average of 79.9% (16 analyses).

Clinopyroxene is the most widely spread mineral typical of all of the gabbro xenoliths (Table 8). In contrast to Cr-diopside, which was found in spinel lherzolite nodules in lavas of Puig de Banya de Boc volcano (Table 8, analyses 1–3), clinopyroxene in xenoliths from the Roca Negra volcano exhibits significant variations in the concentrations of Al2O3 (from 1 to 15 wt at an average of 7.5 wt %) and

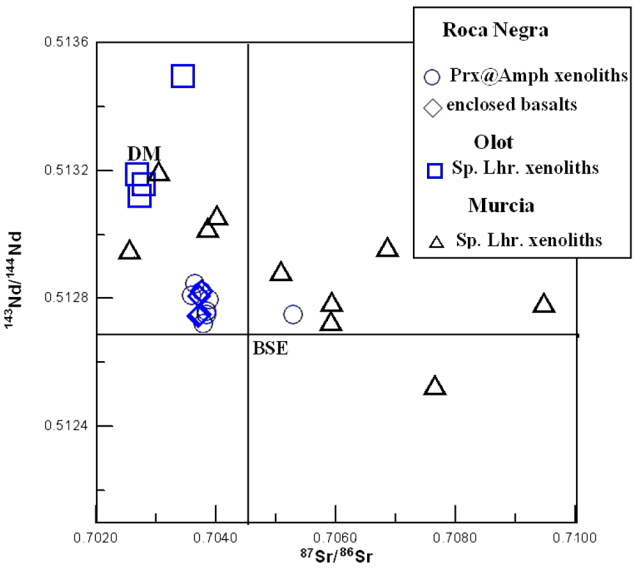

Figure 7. $^{143}Nd/^{144}Nd - ^{87}Sr/^{86}Sr$ diagram for xenoliths of the Roca Negra volcano in comparison with analogous data for lherzolite xenoliths from Cenozoic basalts of Olot [*Bianchini et al.*, 2010) and Murcia (this paper).

TiO_2 (1–3.9 wt % at an average of 1.98 wt %). It is also worth mentioning the variations in the Na_2O concentrations (up to 2.5 wt %). Most of our analyzed clinopyroxenes are titanaugite [*Deer et al.*, 1965).

Orthopyroxene is absent from xenoliths from the Roca Negra volcano and was found only in spinel xenoliths of lherzolite (Puig de Banya de Boc volcano) and gabbro and contains much Al_2O_3 and Cr_2O_3 in the former and only Al_2O_3 in the latter.

Plagioclase varies in composition from $An_{44}Ab_{52}Or_4$ to $An_{89}Ab_{11}$.

Titanomagnetite shows compositional variations similar to those in xenoliths hosted in basalt at Tenerife Island and gabbroids from the Central Atlantic (Table 9). The mineral shows several similarities with titanomagnetite in basalts in the Baikal-Mongolia area [*Lykov et al.*, 1981].

Discussion

In interpreting our results, it is important to consider the composition of the host basalt. As was demonstrated in [*Grachev*, 2003], the basalts are rich in TiO_2 (> 2.5 wt %), FeO^* (> 11 wt %), and MgO (> 10 wt %) and can be classed with Fe–Ti basalts typical of mantle plumes [*Grachev*, 2000]. With regard for the insignificant thickness of the Neogene-Quaternary rocks, the geodynamic environment of volcanism in the Olot area corresponds to a pre-rifting regime. In other areas of pre-rifting regime, xenoliths in basalts are usually dominated by spinel lherzolite and harzburgite [*Grachev*, 2003; *Grachev et al.*, 1981], and pyroxenite xenoliths are practically absent (their content never exceeds a few percent).

Xenoliths in the Roca Negra volcano have anomalous compositions of both their whole-rock samples and their rock-forming minerals, particularly considering the fact that basalts around the Roca Negra volcano ubiquitously contain lherzolite and harzburgite [*Bianchini et al.*, 2007; *Oliveras and Galán*, 2006] but do not bear either phlogopite or amphibole.

Moreover, the unusual chemical composition of the xenoliths (Table 2) is also highlighted by the absence of normative leucite and the practical absence of modal olivine. The Sr and Nd isotopic ratios of the xenoliths and their host basalts (Table 10, Figure 7) are practically exactly identical: $^{87}Sr/^{86}Sr - 0.70359 - 0.703880$, $^{143}Nd/^{144}Nd - 0.512742 - 0.512847$, which testifies that all of them originated from the

Table 10. Sm–Nd and Rb–Sr Isotopic Data on Basalts and Xenoliths From the Roca Negra Volcano, Catalonia

No.	Sample	Sm*	Nd*	Rb*	Sr*	$^{147}Sm/^{144}Nd$	$^{143}Nd/^{144}Nd \pm 2\sigma$	$^{87}Rb/^{86}Sr$	$^{87}Sr/^{86}Sr \pm 2\sigma$
					Xenoliths				
	RC-88-1x								
1	biotite	0.046	0.351	426.9	106.7	0.08450	0.512762 ± 42	11.57366	0.70384 ± 13
2	diopside	5.58	30.52	1.79	184.4	0.11058	0.512722 ± 5	0.02801	0.703776 ± 11
	RC-88-10								
3	diopside	9.851	41.45	5.642	466.6	0.14366	0.512751 ± 3	0.03497	0.705280 ± 15
	RC-88-11								
4	hornblende	6.93	27.25	11.37	508.2	0.15371	0.512811 ± 6	0.06468	0.703589 ± 25
5	diopside	5.72	20.19	12.95	83.5	0.17129	0.512798 ± 6	0.44834	0.703880 ± 28
6	RC-88-3x, whole rock	5.69	22.84	9.69	279.9	0.15099	0.512847 ± 5	0.10015	0.703646 ± 14
7	RC-88-4x, whole rock	0.615	3.147	3.48	456.8	0.14366	0.512751 ± 3	0.03497	0.705280 ± 15
8	RC-88-7x, whole rock	7.744	36.24	21.36	797.5	0.12915	0.512752 ± 5	0.07745	0.703829 ± 11
9	RC-88-8x, whole rock	6.03	23.45	17.78	308.6	0.15210	0.512824 ± 6	0.16861	0.703751 ± 13
					Basalts				
10	RC-88-3b	6.92	37.15	23.41	873.2	0.11290	0.512809 ± 9	0.07759	0.703707 ± 14
11	RC-88-8b	8.08	44.22	38.73	931.1	0.11082	0.512747 ± 12	0.12027	0.703688 ± 15
12	RC-88-12b	10.22	61.60	70.49	1075	0.10060	0.512752 ± 5	0.18950	0.703722 ± 20

*Concentrations of Sm, Nd, Rb, and Sr are in ppm

same mantle (plume) source. At the same time, the Sm–Nd diagram (Figure 8) shows that the composition of xenoliths of the Roca Negra volcano lie within the field of the plume component.

The $^3He/^4He$ isotopic ratios of the xenoliths and their host basalt vary from 0.1 to 3.7×10^{-6} (Table 11)and suggest a strongly degassed source. Higher ratios, as those typical of MORB, were determined in olivine megacrysts in the Roca Negra basalt and spinel lherzolite from Puig de Banya de Boc volcano.

The crystallization parameters of the xenoliths were estimated at 820–1050°C and 6–8 kbar by the amphibole geothermobarometer [*Ernst and Liu*, 1998]. Closely similar values were obtained for the Roca Negra xenoliths in [*Llobera Sanchez*, 1983; *Neumann et al.*, 1999]. It follows from these data that the depth level from which xenoliths were brought

Table 11. He and Ar Isotopes in Xenoliths and Enclosed Basalts of the Roca Negra and Puig de Banya de Boc Volcanoes

No.	Sample	Rock, mineral	^4He, cm^3/g, 10^{-8}	$^3He/^4He$, 10^{-6}	^{40}Ar, cm^3/g, 10^{-8}	$^{40}Ar/^{36}Ar$
			the Roca Negra			
1	RC-10	pyroxenite	2	0.20	98	370
2	RC-10b	basalt	2	0.24	65	300
3	RC-11/3	pyroxenite	3	0.35	50	330
4	RC-12/3	basalt	6	0.10	90	360
5	RC-12/3	basalt	2	0.1	64	430
6	RC-12/2	basalt	1	0.03	50	297
7	RC-12/1	basalt	5	0.14	42	340
			Puig de Banya de Boc			
8	RC-10/5	lherzolite	8	9.5	92	490
9	RC-12/1	Ol*	4	9.4	7	730
10	RC-12	Ol*	3	11.0	17	376
11	RC-1/11	Ol*	8	9.5	37	1947

Note: * – megacrysts in basalt

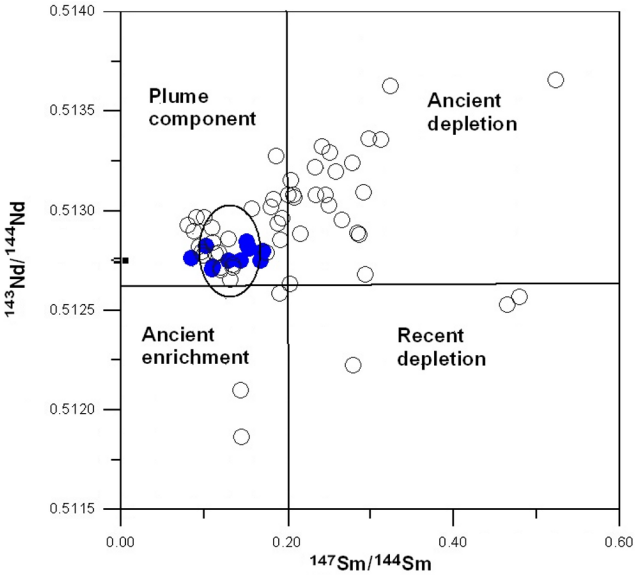

Figure 8. Sm–Nd diagram for the Roca Negra volcano xenoliths in northern Eurasia. The heavy line contours the composition of the continental mantle beneath Europe (according to [*Downes*, 2001]).

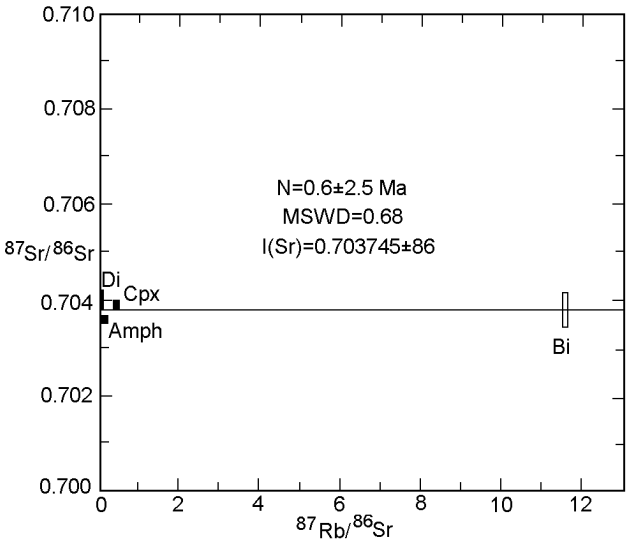

Figure 9. Rb–Sr isochron for xenoliths of the Roca Negra volcano.

to the surface by basalt of the Roca Negra volcano was no greater than 30 km, i.e., was near the mantle–crust boundary.

If basaltic volcanism in the Olot area is of plume nature (the rocks are rich in Mg, Fe, and Ti), then the basaltic melts should have been derived at a temperature of no less than 1400°C and pressure of at least 15 kbar [*White and MacKenzie*, 1989], i.e., at parameters principally different from those of crystallization of the xenoliths of the Roca Negra volcano.

It is also important that the Lu–Hf model age of spinel lherzolite xenoliths in the Olot area is no younger than 600 Ma [*Bianchini et al.*, 2007], whereas the K–Ar mica age of sample RC88-1x is 3.5 Ma, and the Rb–Sr mineral isochron of samples RC88-1x and RC88-11 yields an age of 0.6 ± 2.5 Ma (Figure 9), which corresponds to the age of the metasomatic process.

All data presented above show that xenoliths of the Roca Negra volcano cannot be cumulus rocks, as was thought previously [*Llobera Sanchez*, 1983; *Neumann et al.*, 1999].

We suggest that the rocks found in xenoliths of amphibole and mica pyroxenite hosted in basalts of the Roca Negra volcano were formed by metasomatism at underplating (the development of a high-velocity layer in the bottom portion of the crust), as is typical of mantle plumes. The metasomatic process was driven by fluid enriched in K and P, as follows from Factor 2 $K_{86}P_{81}$, whose loading is 22.6% (Table 3). Experimental data indicate that the intensity of metasomatic transformations depends on the distance between the metasomatized rocks and the fluid source [*Sen and Dunn*, 1994], which explains why these transformations occur only locally in the lower crust beneath the Roca Negra volcano.

Xenoliths of the Roca Negra volcano are obviously unique, and it would be important to elucidate as to whether nodules of such composition are contained in basalts in other areas of intraplate magmatism.

Acknowledgments. The author thanks the Administration of the National Park of the Garrotxa Volcanic Area and its Director Josep Mallarach for providing samples of xenoliths from the Roca Negra volcano for this study. Dr. Juan Marti is thanked for assistance in collecting rock samples.

References

Ancochea, E., P. H. Nixon (1987), Xenoliths in the Iberian Peninsula, *Mantle xenoliths, P. H. Nixon (ed.)* p. 119–124, John Wiley & Sons Ltd, London.

Arana, V., et al. (1983), El volcanismo neogene-cuaternario de Catalunya: caracteres estrcturales, petrologicos y geodinamicos, *Acta Geol. Hispanica*, *18,* 1–17.

Becker, H., T. Wenzel, F. Volker (1999), Geochemistry of glimmerite veins in peridotites from Lower Austria – implications for the origin of K-rich magmas in collision zones, *J. Petrol.*, *40,* 315–338.

Bianchini, G., L. Beccaluva, C. Bonadiman, G. Nowell, et al. (2007), Evidence of diverse depletion and metasomatic events in harzburgite-lherzolite mantle xenoliths from the Iberian plate (Olot, NE Spain): Implications for lithosphere accretionary processes, *Lithos*, *94,* 25–45. doi:10.1016/j.lithos.2006.06.008

Bianchini, G., L. Beccaluva, C. Bonadiman, G. Nowell, et al. (2010), Mantle metasomatism by melts of HIMU piclogite components: new insights from Fe-lherzolite xenoliths (Calatrava Volcanic District, central Spain), *Petrological Evolution of the European Lithospheric Mantle, M. Coltorti, H. Downes, M. Gregoire, S. Y. O'Reilly (eds.), Special Publication 337* p. 107–124, Geological Society, London. doi:10.1144/sp337.6

Boyd, F. R., O. A. Meyer, Eds. (1979), *The Mantle Sample: Inclusions in Kimbrlites and Other Volcanics*, 424 pp., AGU, Washington.

Cameron, K. L., et al. (1992), Contrasting style of precenozoic crustal evolution in Northern Mexico: evidence from deep crustal xenoliths from La Olivina, *J. Geophys. Res.*, *97,* 17353–17376. doi:10.1029/92JB01493

Catalan, M., J. M. Davila (2001), Data gathered to map magnetic anomalies of Spanish sea floor, *EOS*, *82,* 433–435. doi:10.1029/01EO00263

Cebria, J. M., J. Lopez-Ruiz, M. Doblas, R. Oyarzun, et al. (2000), Geochemistry of the Quaternary alkali basalts of Garrotxa (NE volcanoc province, Spain): a case of double enrichment of the mantle lithosphere, *J. Volcan. Geotherm. Res.*, *102,* 217–235. doi:10.1016/S0377-0273(00)00189-X

Conticelli, S. (1998), The effect of crustal contamination on ultrpotassic magmas with lamproitic affinity: mineralogical, geochemical and isotope data from the Torre Alfina lavas and xenoliths, Central Italy, *Chemical Geology*, *149,* 51–81. doi:10.1016/S0009-2541(98)00038-2

Coy-Yll, R., B. M. Gunn, A. Traveria-Cross (1974), Geochemisrty of the Catalonian volcanics, Spain, *Acta Geol. Hispanica*, *IX,* 127–132.

Danchin, R. V. (1979), Mineral and bulk chemistry of lherzolite and garnet xenoliths from the Premier mine, *The mantle samples: inclusions in kimberlites and others volcanics, F. R. Boyd and O. A. Meyer (eds.)* p. 104–126, AGU, Washington. doi:10.1029/SP016p0104

Dawson, J. B. (1972), Kimberlites and their relation to the mantle, *Phil. Trans. R. Soc. Lond.*, *A. 271,* 297–311. doi:10.1098/rsta.1972.0011

Dawson, J. B., J. V. Smith (1977), The MARID (mica-amphibole-ritile-ilmenite-diopside) suite of xenoliths in kimberlite, *Geochim. Cosmochim. Acta*, *41,* 309–323. doi:10.1016/0016-7037(77)90239-3

Deer, W. A., R. A. Howie, J. Zusmann (1965), *Rock-Forming Minerals, 3. Sheet Silicates*, Wiley, New York.

Dobretsov, G. L., T. L. Dobretsova (1975), Deep nodules in basaltoids and alkaline gabbroids in continents: Kazakhstan and the northern Tien Shan, *Deep Xenoliths and the Upper Mantle* p. 118–125, Nauka, Novosibirsk.

Dobretsov, N. L., V. S. Sobolev, N. V. Sobolev (1975), Mineralogical specifics of deep nodules, *Deep Xenoliths and the Upper Mantle* p. 205–216, Nauka, Novosibirsk.

Donville, D. (1973), *Geologie Neogene et Ages des Eruptions Volcaniques de la Catalogne Orientale. These le Grade de Docteur es Sciences Naturelles*, 133 pp., L'Universite Paul Sabayier, Noulouse.

Downes, H. (2001), Formation and modification of the shallow sub-continental lithospheric mantle: A review of geochemical evidence from ultramafic xenolith suites and tectonically emplaced ultramafic massifs of western and Central Europe, *J. Petrol.*, *42,* 233–250. doi:10.1093/petrology/42.1.233

Ernst, W. G., J. Liu (1998), Experimental phase-equilibrium study of Al- and Ti-contents of calcic amphibole in MORB: A semiquantitative barometer, *American Mineralogist*, *83,* 952–969.

Frisch, T., Y. U. Schminke (1970), Petrology of clinopyroxene-amphibole inclusions from the Roque Nublo volcanics, Gran Canaria, Canary islands, *Bull. Volcanologique*, *XXXIII,* 1073–1088.

Gallart, J., C. Olivera, A. Correig (1984), Aproximacion geofisica a la zona volcanica de Olot (Girona). Estudio local de sismicidad, *Rev de Geofisica*, *40,* 205–226.

Giannetti, B., J. F. Luhr (1990), Phlogopite-clinopyroxenite nodules from high-K magmas, Roccamonfina Volcano, Italy: Evidence for a low-pressure metasomatic origin, *Earth Planet. Sci. Lett.*, *101,* 404–424. doi:10.1016/0012-821X(90)90169-X

Grachev, A. F. (2000), Areas of pre-rifting regime: general characteristics, *Modern Tectonics, Geodynamics, and Seismicity of North Eurasia* p. 139–141, Probel, Moscow.

Grachev, A. F. (2003), Final volcanism in Europe and its geodynamic nature, *Physics of the Earth*, No. 8, 11–46.

Grachev, A. F., E. V. Devyatkin (1997), Pre-rifting tectonic regime, *Geology and Management of Subsurface*, No. 1, 4–10.

Grachev, A. F., A. N. Komarov (1994), The new data on the uranium content in the continental and oceanic mantle, *Physics of the Solid Earth*, *30,* 1–8.

Grachev, A. F., Yu. S. Genshaft, A. Ya. Saltykovskii (1981), Geodynamics of the Baikal-Mongolia region in the Cenozoic, *Comprehensive Studying the Development ofthe Baikal-Mongolia Region in the Cenozoic* p. 134–176, IFZ AN SSSR, Moscow.

Ikorsky, S. V., I. L. Kamensky (1998), Crushung of rocks and minerals in glass ampullae under the noble gases isotope study, *Isotope Geochemistry, 15 Symposium, Abstracts* p. 115, Vernadsky Institute geochemistry, Moscow.

Ionov, D., S. Borisovskii, V. Kovalenko, I. Ryabchikov (1984), First find of amphibole in deep xenoliths hosted by alkaline basalt in Mongolia, *Dokl. AN SSSR*, *276,* 238–242.

Ionov, D. A., A. W. Hofmann (1995), Nb-Ta-rich mantle amphiboles and micas: Implications for subduction-related metasomatic trace element fractionations, *Earth Planet. Sci. Lett.*, *131,* 341–356. doi:10.1016/0012-821X(95)00037-D

Kamensky, I. L., I. N. Tolstichin, V. R. Vetrin (1990), Juvenile helium in ancient rocks: ^{3}He excess in amphibolites from 2.8 Gacharnokite series – crust mantle fluid in intracrustal magmatic processes, *Geochim. et Cosmochim. Acta*, *54,* 3115–3122. doi:10.1016/0016-7037(90)90127-7

Kaneoka, I., N. Takaoka, K. Aoki (1978), *Terrestrial Rare Gases*, 71–83 pp., Japan Sci. Soc. Press, Tokyo.

Kogarko, L. N. (1990), Geochemistry of magmatic rocks, *Tectonics and Magmatism of the Cape Verde Islands* p. 157–212, Nauka, Moscow.

Lasko, E. E., E. E. Sharkov, Eds. (1988), *Magmatic Rocks, Vol. 5. Ultramafic Rocks*, 508 pp., Nauka, Moscow.

Llobera Sanchez, P. (1983), Petrlogia de los enclaves del volcan the Roca Negra (Olot, NE Espana), *Estud. Geol.*, *41,* 105–126.

Lopez Ruiz, J., E. Rodrigues Badiola (1985), La region volcanica mio-pleistocena del NE de Espana, *Estud. Geol.*, *41,* 105–126. doi:10.3989/egeol.85413-4696

Losantos, M., E. Aragone's, X. Bera'stegui, J. Palau, et al. (1989), Mapa geologic de Catalunya, scale 1:25,0000, Serv. Geol. de Catalunya, Barcelona.

Lykov, A. V., D. M. Pecherskii, Z. V. Bragina (1981), Magnetic properties of Pliocene-Quaternary basalts and xenoliths in Mongolia, *Comprehensive Studying the Development of the Baikal-Mongolia Region in the Cenozoic* p. 101–116, IFZ AN SSSR, Moscow.

MacGregor, I. D. (1979), Mafic and ultrmafic xenoliths from the Kao kimberlite pipe, *The Mantle Samples: Inclusions in Kimberlites and Others Volcanics, F. R. Boyd and O. A. Meyer (eds.)* p. 156–182, AGU, Washington. doi:10.1029/SP016p0156

Mallarach, J. M., M. Riera (1981), *Els Volcans Olotins el Seu Paisatge*, 250 pp., Sepra, Barcelona.

McDonough, W. F., S.-S. Sun (1995), The composition of the Earth, *Chem. Geol.*, *120,* 223–253. doi:10.1016/0009-2541(94)00140-4

Marti, J., J. Mitjavila, A. Aparicio, E. Roca (1992), Cenozoic magmatism in the Valencia trough, *Tectonophysics*, *203,* 145–165.

Melyakhovitskii, A. A., I. V. Ashchepkov, B. P. Yudin (1988), Mantle metasomatites and related nodules in basaltoids from the Barkoiskie volcanoes, *Geology and Geophysics*, No. 9, 24–34.

Montoto, M., R. M. Esbert (1967), Estudio petrologico de la zona basaltica de Hostarlich (Gerona), *Rev. Inst. Inv. Geol. Deputacion Prov. Barcelona*, *21,* 11–35.

Mouchketoff, D. (1928), Role et valeur de la region volcanigue Catalane dans la conception de la tectonique du littoral de la Mediterranee occidentale, *Geologie Mediterranee Occid.*, *II,* No. 26, 3–8.

Munoz, M., J. Sagredo, A. Afonso (1974), Mafic and ultramafic inclusions in the eruption of Teneguia volcano (La Palma, Canary islands), *Estudios Geologicos*, *Vol. Teneguia,* 65–74.

Neumann, E.-R., J. Marti, J. Mitjavila, E. Wulff-Pederson (1999), Origin and implications of mafic xenoliths associated with Cenozoic extension-related volcanism in the Va-

lencia Trough, NE Spain, *Miner. Petrol.*, *65,* 133–139. doi:10.1007/BF01161579

Oliveras, V., G. Galán (2006), Petrologia y mineralogia de los xenolitos mantélicos del volcán la Banya del Boc (Girona), *Geogaceta*, *40,* 107–110.

Reid, A. M., A. P. Le Roex (1988), Kaersutite-bearing xenoliths and megacrysts in volcanic rocks from the Funk seamount in the southwest Indian ocean, *Mineral. Mag.*, *52,* 359–370. doi:10.1180/minmag.1988.052.366.07

Richard, P., N. Shimuzu, C. J. Allegre (1976), $^{143}Nd/^{144}Nd$ a natural tracer. An application to oceanic basalts, *Earth Planet. Sci. Lett.*, *31,* 269–378. doi:10.1016/0012-821X(76)90219-3

Sagredo, J. (1969), Origen de la inclusiones de dunitas y otras ultramaficas en las rocas volcanicas de Lanzarote y Fuerteventura, *Estud. Geol.*, *XXY,* 189–233.

Sen, C., T. Dunn (1994), Experimental modal metasomatism of a spinel lherzolite and the production of amphibole-bearing peridotite, *Contrib. Mineral. Petrol.*, *119,* 422–432. doi:10.1007/BF00286939

Tournon, J. (1968), Les roches basaltiques de la province de Gerone (Espagne) basanites a leucite et basanites a analcime, *Bull Soc. Fr. Mineral. Cristallogr.*, *92,* 376–382.

White, R., D. McKenzie (1989), Magmatism at Rift Zones: the Generation of Volcanic Continental Margins and Flood Basalts, *J. Geophys. Res.*, *94,* 7685–7730. doi:10.1029/JB094iB06p07685

Witt, G., H. A. Seck (1989), Origin of amphiboles in recrystallized and porphyroclastic mantle xenoliths from the Rhenish Massif: implications for the nature of mantle metasomatism, *Earth Planet. Sci. Lett.*, *91,* 327–340. doi:10.1016/0012-821X(89)90007-1

Zharikov, V. A., A. F. Grachev, eds. (1987), *Mantle Xenoliths and the Structure of the Lithosphere*, 239 pp., Nauka, Moscow.

A. F. Grachev, Schmidt Institute of Physics of the Earth, Russian Academy of Sciences, 10 Bolshaya Gruzinskaya, Moscow, Russia. (afgrachev@gmail.com)